

## Measurement of Dynamic Soil Water Content Based on Electrochemical Capacitance Tomography

Muhammad Mukhlisin<sup>1,2,\*</sup>, Almushfi Saputra<sup>1</sup>, Ahmed El-Shafie<sup>1</sup> and Mohd. Raihan Taha<sup>1</sup>

<sup>1</sup> Department of Civil and Structural Engineering, Faculty of Engineering and Built Environment, Universiti Kebangsaan Malaysia

<sup>2</sup> Department of Civil Engineering, Polytechnic Negeri Semarang, Indonesia

\*E-mail: [mmukhlis2@yahoo.com](mailto:mmukhlis2@yahoo.com)

*Received:* 8 February 2012 / *Accepted:* 29 April 2012 / *Published:* 1 June 2012

---

In this study a new model for the relationship of normalized volumetric water content and relative permittivity relationship have been proposed. Electrical Capacitance Volume Tomography (ECVT) was applied to image soil water content during infiltration of water in a soil column based on the proposed model. Granular and silty sand were used as soil material in the experiments. The principle of normalization in measurements of permittivity in ECVT is required to determine normalized volumetric soil water content. This technique utilizes the distribution of normalized relative permittivity in the voxel to analyze the volume of each voxel that contains of water. The result showed that the normalized volumetric water content can be seen in each layer during soil water infiltration in the soil column.

---

**Keywords:** Normalized volumetric water content; electrical capacitance volume tomography; relative permittivity

### 1. INTRODUCTION

It is widely accepted that soils are useful for various studies area. For example in agriculture study, measurement of water content of soil is required to determine water source and ensure the quality of crop [1]. Moreover, soil water content is useful to analyze soil water contamination by observing changes in water content during the addition of substance [2]. Soil water content also plays an important role in slope stability analysis [3-6].

Various techniques in the measurement of contamination and water content of soil have been discussed in literatures (e.g., [7-12]). Based on previous studies, soil-water content measurement techniques are widely used is an electromagnetic method [13] such as Time domain Reflectometry

(TDR) [14], Ground Penetrating Radar (GPR) [8], and Electrical Capacitance [15]. These all methods measure the value of relative permittivity of soil to find soil water content.

Tomography is a promising technique for measurement of water content in soil, especially for capacitance-based tomography. This is due to the technique is not only capable of measuring water content in the soil, but also capable to image the distribution of water in the soil. Tomography technique is also preferred because it is non-destructive and non-invasive system. As a tomography technique, ECVT is a system used to view enclosed objects by measuring changes in capacitance then compute relative permittivity distribution to create three dimension images in real-time [16]. Shape of geometry sensor on ECVT not confined to one form of shape, it can be in the form of arbitrary shape of geometries [17]. This possibility gives an extra advantage of ECVT in measuring soil water content.

The previous study has successfully monitored the propagation of distribution of water in soil column [18]. In this study, the equation of normalized volumetric water content was proposed and then compared with the previous model proposed by Topp et al [20], Roth [21] and Malicki [22]. The proposed model was then used to analyze the volumetric water content during soil water infiltration in a soil column based on ECVT monitoring system.

## 2. MATERIAL AND METHODS

### 2.1. ECVT Principle

Basic measurement of ECVT derived from Poisson's equation

$$\nabla \cdot (\varepsilon(x, y, z) \nabla \phi(x, y, z)) = -\rho(x, y, z) \quad (1)$$

where  $\varepsilon$  is relative permittivity distribution,  $\phi$  is electric potential, and  $\rho$  is charge distribution. From Eq. 1, capacitance value can be obtained by using the equation below

$$C = \frac{1}{\Delta V} \oint_{\Gamma} \varepsilon(x, y, z) \nabla \phi(x, y, z) \cdot \hat{n} \, dl \quad (2)$$

where  $V$  is potential difference and  $C$  is capacitance. By using matrix expression, Eq.2 can be written like the following equation

$$\mathbf{C} = \mathbf{S} \mathbf{G} \quad (3)$$

where  $C$  is capacitance matrix,  $G$  is distribution of relative permittivity matrix and  $S$  is sensitivity matrix. The sensitivity matrix generate from sensor and geometry design and number of sensors. In matrix operation the value of  $G$  can be obtained by inverse the matrix of  $S$  and multiply it with matrix  $C$ . For non-square matrix, matrix inversion is very difficult to solve, so the approximation could be attempted by using transpose matrix. The equation for calculate matrix  $G$  becomes

$$\mathbf{G} = \mathbf{S}^T \mathbf{C} \quad (4)$$

The Eq. 3 and Eq. 4 are known as the forward and inverse problem respectively. Inverse problem was used to reconstruct the capacitance measurements become relative permittivity distribution. The simple method for reconstruction used linear back projection (LBP) [19].

## 2.2. Soil Water Content and Relative Permittivity Relationship

The relationship between relative permittivity and volumetric water content has been used by previous researchers to determine the volumetric water content. Various equations have been presented to show the relationship between relative permittivity and volumetric water content. The common-well empirical relationship was proposed by Topp et al [20] is shown below

$$\theta = -5.3 \times 10^{-2} + 2.92 \times 10^{-2} \varepsilon - 5.5 \times 10^{-4} \varepsilon^2 + 4.3 \times 10^{-6} \varepsilon^3 \quad (5)$$

where  $\varepsilon$  is relative permittivity and  $\theta$  is volumetric water content.

The other equation proposed by Roth [21] which used the principle of mixing model, as shown below

$$\varepsilon = \left( (1-\eta)\varepsilon_s^\gamma + \theta\varepsilon_w^\gamma + (\eta-\theta)\varepsilon_a^\gamma \right)^{1/\gamma} \quad (6)$$

where  $\varepsilon_s$ ,  $\varepsilon_w$ , and  $\varepsilon_a$  are the relative permittivity of soils, water and air, respectively (see Table 1).  $\eta$  is porosity of soil.  $\gamma$  value varies between -1 (for three phase in series) to 1 (for three phase in parallel). If the value of  $\gamma$  is one, then Eq. 6 becomes

$$\theta = \frac{\varepsilon - (1-\eta)\varepsilon_s - \eta\varepsilon_a}{\varepsilon_w - \varepsilon_a} \quad (7)$$

Malicki [22] proposed the equation for permittivity and volumetric water content that covers mineral and organic soil.

$$\theta = \frac{\sqrt{\varepsilon - 3.47 + 6.22\eta - 3.82\eta^2}}{7.01 + 6.89\eta - 7.83\eta^2} \quad (8)$$

## 2.3. Normalization Method

In this study the relative permittivity was analyzed by the ECVT system generates in the form of normalization. Normalized volumetric water content,  $\Theta$ , can be defined as

$$\Theta = \frac{\theta - \theta_r}{\theta_s - \theta_r} \tag{9}$$

where  $\theta$  is the volumetric water content,  $\theta_r$  is the residual volumetric water content, and  $\theta_s$  is the saturated volumetric water content.

The normalization of relative permittivity gives privilege to define normalized volumetric water content. In this study three models are proposed as in Eq. 10(a), 10(b) and 10(c).

$$\begin{aligned} \Theta &= \varepsilon_N^{0.5} & \text{(a)} \\ \Theta &= \varepsilon_N & \text{(b)} \\ \Theta &= \varepsilon_N^2 & \text{(c)} \end{aligned} \tag{10}$$

where  $\varepsilon_N$  is normalized permittivity which can be calculated as

$$\varepsilon_N = \frac{\varepsilon - \varepsilon_{drysoil}}{\varepsilon_{saturatedsoil} - \varepsilon_{drysoil}} \tag{11}$$

where  $\varepsilon$ ,  $\varepsilon_{dry\ soil}$  and  $\varepsilon_{saturated\ soil}$  are actual relative permittivity measurement, relative permittivity of dry soil and relative permittivity of saturated soil, respectively. Substituted Eq. 11 to Eq. 10 result Eq. 12(a), 12(b) and 12(c) as proposed model 1, model 2 and model 3, respectively.

$$\begin{aligned} \Theta &= \left( \frac{\varepsilon - \varepsilon_{drysoil}}{\varepsilon_{saturatedsoil} - \varepsilon_{drysoil}} \right)^{0.5} & \text{(a)} \\ \Theta &= \left( \frac{\varepsilon - \varepsilon_{drysoil}}{\varepsilon_{saturatedsoil} - \varepsilon_{drysoil}} \right) & \text{(b)} \\ \Theta &= \left( \frac{\varepsilon - \varepsilon_{drysoil}}{\varepsilon_{saturatedsoil} - \varepsilon_{drysoil}} \right)^2 & \text{(c)} \end{aligned} \tag{12}$$

The value of relative permittivity air, water, dry soil and saturated soil can be seen in Table 1. Relative permittivity of dry soil and saturated soil are obtained from the study of the previous researchers [23]. Relative permittivity of material is affected by the chemical components of its constituent and can be calculated by using the mixture model [24].

**Table 1.** Relative permittivity of material properties

Material	Relative Permittivity	Chemical Elements
Air ( $\varepsilon_{air}$ )	1	N <sub>2</sub> , O <sub>2</sub>
Water ( $\varepsilon_{water}$ )	80	H <sub>2</sub> O
Dry Soil ( $\varepsilon_{dry\ soil}$ )	2-4	N, P, K, Ca, Mg, S, Cu, Zn, Fe, Mn, B, Cl, Na, H
Saturated Soil ( $\varepsilon_{saturated\ soil}$ )	23-28	H <sub>2</sub> O, N, P, K, Ca, Mg, S, Cu, Zn, Fe, Mn, B, Cl, Na, H

#### 2.4. Experimental Setup

ECVT system consists of three part (i) sensors, (ii) data acquisition, and (iii) system reconstruction and visualization, as shown in Fig. 1. In this experiment 32 and 24 channels hexagonal sensors were used for the first and second experiments, respectively. Moreover the heights of soil column for the first and second experiments are 32 and 27cm, respectively and 11.5cm in diameters. The both of experiments are divided into 32 layers with the 1<sup>st</sup> layer in the top of column and go down up to 32<sup>rd</sup> layer located at the bottom of column.

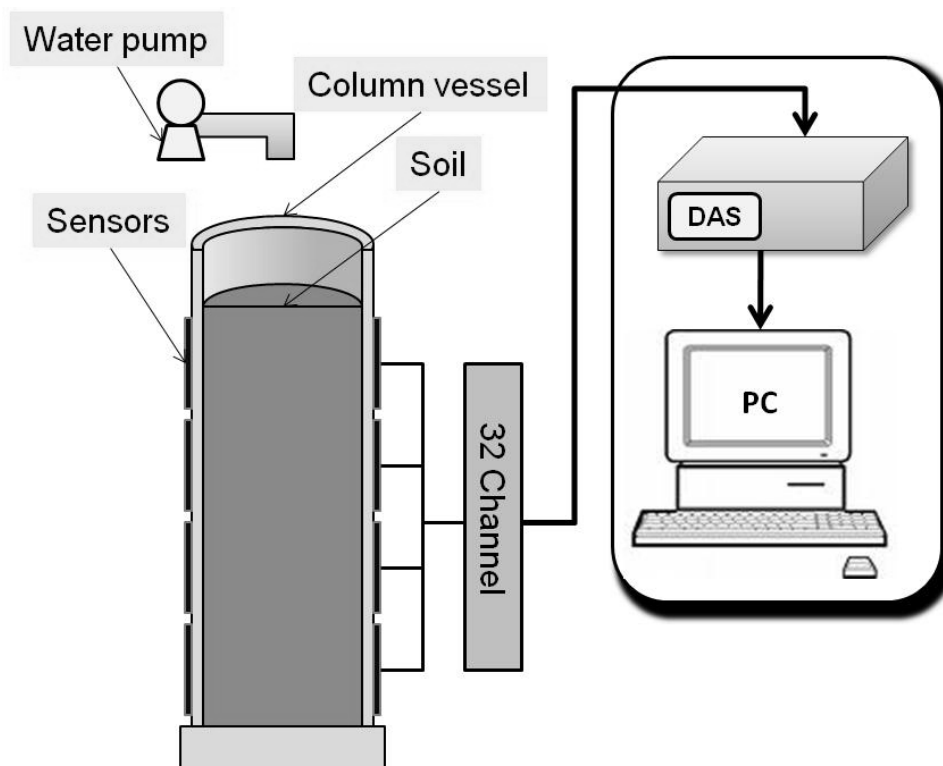


**Figure 1.** Experimental setup [18]

In the first experiment, 3 liter by volume of soil in the column was supplied. The soil material used in this study was sand collected from the Cisadane river in Tangerang, Indonesia. The soil contained 17 % fine sand and 83 % medium sand with porosity of soil 41.79%. The specific gravity and soil density were 2.663 and 1.55 g cm<sup>-3</sup>, respectively. In this experiment, the soil in the vessel was supplied with water flow with a discharge 7.2 ml/s until ponded condition and the discharge was stopped when the pond of water level at 2 cm above the surface soil. During ponded condition, the data capacitances were measured iteratively and sent to the computer. The data acquisition frequency was set to one frame per second.

In the second experiment, 3 kg of silty sand was supplied into the column. After that, 1.4 liter of water was filled into the soil column using constant head method, which height of the water was maintained constant at 4 cm above the surface of soil.

### 3. RESULT AND DISCUSSION

#### 3.1. Normalization Result

Eq. 5, 7, 8 and 12 are plotted in a graph with the concept of normalization. Data of dry and saturated soil permittivity in Table 1 is used to calculate the approximate value of residual water content and saturated water content by using Eq. 5, 7 and 8. After obtaining the residual and saturated water content, normalized volumetric water content can be calculated using Eq. 9

Fig. 2 shows the relationship between normalized volumetric water content and relative permittivity for Eq. 5, 7, 8 and 12. The figure shows that the Malicki's [22] and Topp's [20] model in terms of normalized volumetric water content merged perfectly with the model 1. Whereas, Roth model [25] are also fit very well with the model 2. Data of Topp [20] and Roth [25] are plotted in Fig. 2. By assuming the minimum and maximum value of data are the residual and saturated water content, respectively then the value of normalized water content can be calculated. In addition, the Roth [25] data actually was used by Malicki [22] to calibrate the permittivity and water content relationship which kind of mineral soil with bulk density  $1.4\text{g/cm}^3$ . Data of Topp [20] is from the type of vermiculite with value of dry density  $1.08\text{g/cm}^3$ . The data looks quite fit with Model 1, Topp's model and Malicki's model. This proves that in terms of normalization, the form of equation can be further simplified and has the potential to determine the relationship between relative permittivity and water content in soil.

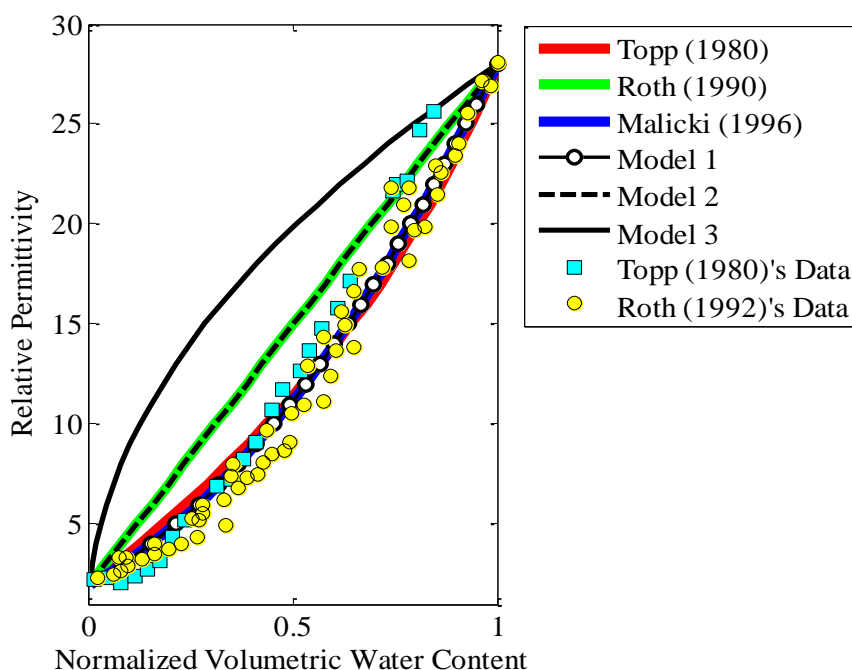


**Figure 2.** Normalized volumetric water content and relative permittivity relationship of three proposed model compared with established models and data experiments from previous studies.

3.2. Experiment Results

Fig. 2 shows that Eq. 12a as proposed model 1 is a good model to be used to analyze normalized volumetric water content. Based on the result the model 1 was then used to analyze the normalized volumetric water content during water infiltration in soil. The results of water infiltration in soil can be seen in Figs. 4 and 5. Figure 4a shows the images of normalized volumetric water content from red (i.e., dry condition,  $\epsilon_N = 0$ ) to blue (i.e., saturated condition,  $\epsilon_N = 1$ ) colors. The scale of the color means normalization value of relative permittivity distribution in image.

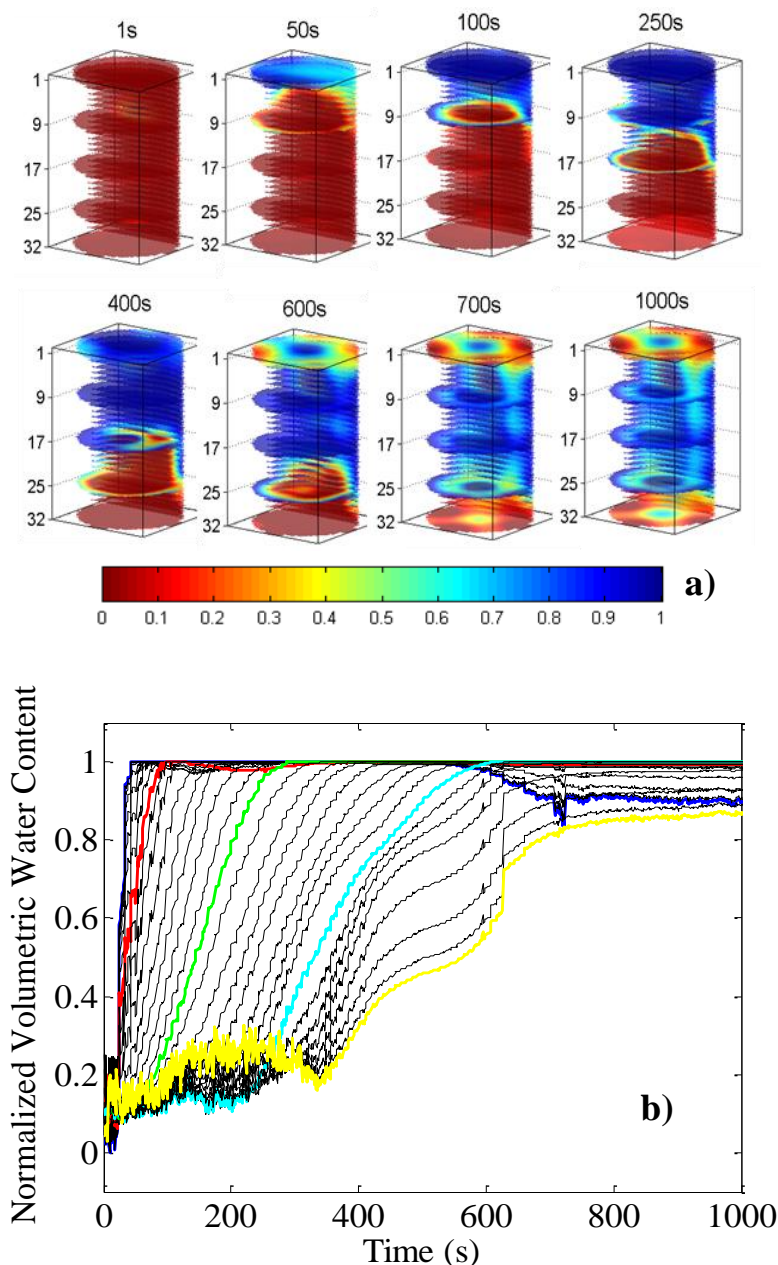


**Figure 4.** Result from experiment 1, (a) soil water infiltration and (b) normalized volumetric water content of soil (blue line 1<sup>st</sup> layer; red line 9<sup>th</sup> layer; green line 17<sup>th</sup> layer; cyan line 25<sup>th</sup> layer; and yellow line: 32<sup>th</sup> layer)

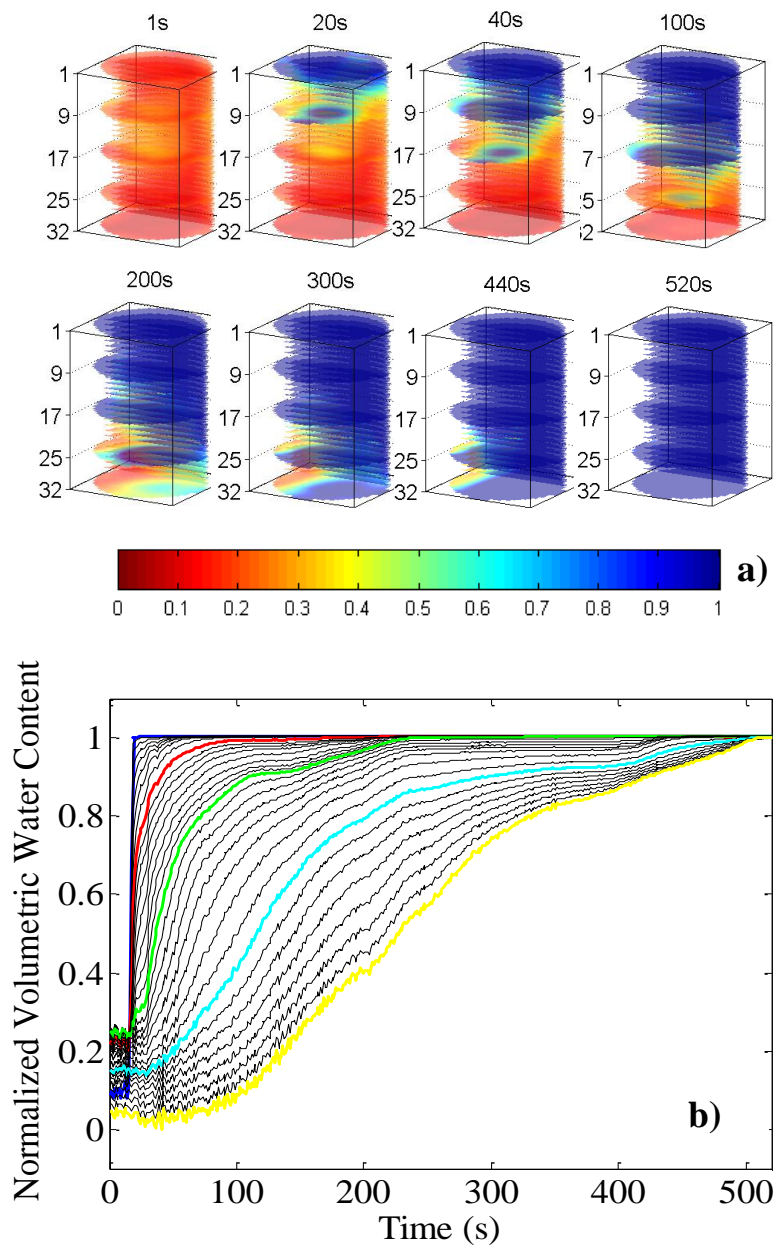


**Figure 5.** Result from experiment 2, (a) soil water infiltration and (b) normalized volumetric water content of soil (blue line 1<sup>st</sup> layer; red line 9<sup>th</sup> layer; green line 17<sup>th</sup> layer; cyan line 25<sup>th</sup> layer; and yellow line: 32<sup>th</sup> layer)

Fig. 4a shows the image sequencing of water infiltration methods from 1, 50, 100, 250, 400, 600, 700 and 1000 seconds, respectively. In this figure, can be seen clearly the position and movement of water per seconds. Fig. 4b shows normalized volumetric water content of soil for 32 layers during water infiltration in the soil. Blue, red, green, cyan and yellow lines indicated 1, 9, 17, 25 and 32 soil layers, respectively. In the first layer the normalized volumetric water content increase very fast and reach to saturated condition at around 50 seconds. Degree of saturation for the 1<sup>st</sup> layer begins to decrease at 600 seconds due to water filling was stopped at that time and the stagnant water on the first layer began to decrease and flow into the lower layer. While the normalized volumetric water content

value of the 32<sup>nd</sup> layer from the first to 350 seconds shows moving in fluctuations. This is probably due to the effect of air movement when the water fills the pores of soil. This experiment showed clearly the availability air trap at the bottom of soil in the vessel (see Fig. 4a).

Fig. 5 also shows the image of soil water infiltration (Fig. 5a) and normalized volumetric water content of each layer of the soil column (Fig. 5b). In Fig. 5a can be seen that the initial value of normalized volumetric water content for the silty sand is at around 0.2 before water infiltrate to the soil column. This is due to the effect initial soil moisture water in the soil. Fig. 5b shows the water infiltrates into the each soil layer. The first layer has increased drastically around in the first 30 seconds, while for the last layer the normalized volumetric water content increases gradually and reach saturated condition at around 500 seconds. The figure shows the mechanism of increasing normalized volumetric water content from 1<sup>st</sup> to 32<sup>nd</sup> from dry to saturated condition during water infiltration in the soil column in 3D using the proposed model 1.

Furthermore, some previous studies have also analyzed the imaging of water infiltration and distribution, such as using the modalities of electrical resistivity tomography [26], X-rays computerized tomography [27], and magnetic resonance imaging (MRI) [28]. Electrical resistivity tomography was able to measure soil water content in three-dimensional image, but depends on the stability of the resistivity of water [26]. Microfocus X-rays CT can measure soil water content with very high resolution (1 $\mu$ m), but it took 2 minutes to 1 hour for reconstruction image [27]. Meanwhile, MRI can image the soil water content with time intervals of 45s for each image, but only in 2-dimensional image [28]. However, the method of measurement of soil water infiltration using ECVT can be done in real time and three-dimensional image.

#### 4. CONCLUSION

The concept of normalization of water content has been discussed and compared. In this study the new model for the relationship of normalized volumetric water content and relative permittivity relationship have been proposed. The proposed model 1 has successfully merged very well with previous model proposed by Malicki's and Topp's. While the proposed model 2 has also perfectly merged with Roth's model. The proposed model has also succeeded to measure the normalized volumetric water content of water infiltration in the soil column using ECVT system. Normalized volumetric water content can be shown and analyzed layer per layer of soil column for every second. We found that The ECVT system has advantages in measuring soil water content including non-destructive and non-invasive to the sample object, 3D image and real-time monitoring for water infiltration.

#### ACKNOWLEDGEMENT

The authors would like to thank M. R. Baidillah for supporting data for this study. This work was supported by grant from Research University Grand (GUP) of Universiti Kebangsaan Malaysia and Fundamental Research Grant Scheme (FRGS) under Ministry of Higher Education (MOHE) of Malaysia.

## References

1. T. Moroizumi, H. Hamada, S. Sukchan and M. Ikemoto, *Agricultural Water Management*, 96 (2008) 160
2. B. D. Kottler, J. C. White and J. W. Kelsey, *Chemosphere*, 42 (2000) 893
3. N. Osman and S. S. Barakbah, *Ecological Engineering*, 28 (2006) 90
4. M. Mukhlisin, M. R. Taha and K. Kosugi, *Geosciences Journal*, 12 (2008) 401
5. M. Mukhlisin, M. R. Taha, *European J. Sci. Res.*, 30 (2009) 36
6. M. Mukhlisin, M. R. Baidillah, M. R. Taha and A. El-Shafie, *Int. J. Phys. Sci.*, 6 (2011) 4629
7. G. C. Topp, *Hydrol. Process*, 17 (2003) 2993
8. J. A. Huisman, S. S. Hubbard, J. D. Redman and A. P. Annan, *Vadose Zone Journal*, 2 (2003) 476
9. J. M. Basinger, G. J. Kluitenberg, J. M. Ham, J. M. Frank, P. L. Barnes and M. B. Kirkham, *Vadose Zone Journal*, 2 (2003) 389
10. G. J. Gaskin and J. D. Miller, *J. agric. Engng Res.*, 63 (1995) 153
11. V. Ramirez, J. A. Sanchez, G. Hernandez, S. Solis, J. Torres, R. Antano, J. Manriquez and E. Bustos, *Int. J. Electrochem. Sci.*, 6 (2011) 1415
12. C. Ruiz, J. M. Anaya, V. Ramirez, G. I. Alba, M. G. Garcia, A. Carrillo-Chavez, M. M. Teutli and E. Bustos, *Int. J. Electrochem. Sci.*, 6 (2011) 548
13. S. Y. Wu, Q. Y. Zhou, G. Wang, L. Yang and C. P. Ling, *Environ Earth Sci*, 62 (2010) 999
14. D. A. Robinson, S. B. Jones, J. M. Wraith, D. Or and S. P. Friedman, *Vadose Zone Journal*, 2 (2003) 444
15. C. M. K. Gardner, T. J. Dean and J. D. Cooper, *J. agric. Engng. Res.*, 71 (1998) 395
16. W. Warsito, Q. Marashdeh and L.S. Fan, *IEEE Sensors Journal*, 7 (2007) 525
17. W. Warsito, Q. Marashdeh and L. S. Fan, *5<sup>th</sup> World Congress on Industrial Process Tomography, Bergen, Norway*, (2007)
18. M. Mukhlisin, M. R. Baidillah, A. El-Shafie, M. R. Taha, and W. Warsito. *Hydrology and Earth System Sciences Discussions*, 9 (2012) 1367
19. W. Q. Yang, D. M. Spink, T. A. York and H. McCann, *Measurement Science and Technology*, 10 (1999) 1065
20. G. C. Topp, J. L. Davis and A. P. Annan, *Water Resour Res*, 16 (1980) 574
21. K. Roth, R. Schulin, H. Fluhler and W. Attinger, *Water Resour Res*, 26 (1990) 2267
22. M. A. Malicki, R. Plagge and C. H. Roth, *Eur J Soil Sci*, 47 (1996) 357
23. D. A. Robinson, S. B. Jones, J. M. Blonquist Jr. and S. P. Friedman, *Soil Sci. Soc. Am. J.*, 69 (2005) 1372
24. Sami Sharif, *IEEE Transactions on Geoscience and Remote Sensing*, 33 (1995) 353
25. C. H. Roth, M. A. Malicki and R. Plagge, *J. Soil Sci.*, 43 (1992) 1
26. Q. Y. Zhou, J. Shimada and A. Sato, *Water Resources Research*, 37 (2001) 273
27. R. Tippkotter, T. Eickhorst, H. Taubner, B. Gredner and G. Rademaker, *Soil & Tillage Research*, 105 (2009) 12
28. M. H. G. Amin, K. S. Richards, R. J. Chorley, S. J. Gibbs, T. A. Carpenter and L. D. Hall, *Magnetic Resonance Imaging*, 14 (1996) 879